J. Physiol. (1987), **384**, *pp.* 649–669
With 10 *text-figures*
Printed in Great Britain

ANALYSIS OF GATED MEMBRANE CURRENTS AND MECHANISMS OF FIRING CONTROL IN THE RAPIDLY ADAPTING LOBSTER STRETCH RECEPTOR NEURONE

BY Å. EDMAN, S. GESTRELIUS AND W. GRAMPP

From the Department of Physiology and Biophysics, University of Lund, Sölvegatan 19, S-223 62 Lund, Sweden

(*Received 24 March 1986*)

SUMMARY

1. The gated membrane currents (a tetrodotoxin-sensitive Na^+ current and a tetraethylammonium- and 4-aminopyridine-sensitive K^+ current) of the rapidly adapting stretch receptor neurone of lobster were investigated with respect to their kinetic properties using electrophysiological, pharmacological, and mathematical techniques.

2. The currents were found to be controlled by slow inactivations as well as by fast Hodgkin–Huxley (1952) gating processes. They could be described by kinetic expressions which differed from those inferred for the slowly adapting receptor (Gestrelius & Grampp, 1983*a*; Gestrelius, Grampp & Sjölin, 1983) only with respect to some of the parameter values.

3. With these expressions, and additional equations for the cell's pump and leak current components (Edman, Gestrelius & Grampp, 1986), a mathematical receptor model was formulated which accurately predicts the impulse activity of the living preparation in different functional circumstances and which, therefore, was adopted as an appropriate theory of firing regulation.

4. From a model analysis it appeared (a) that the 'rapid' adaptation of the receptor's impulse activity is mainly an effect of slow Na^+ current inactivation starting a regenerative process of accommodation which, basically, is due to a small ratio of subthreshold Na^+ to K^+ currents; (b) that, because of the transmembrane Na^+ influx being limited by accommodation, impulse firing is only little affected by a Na^+-dependent pump current activation; and (c) that the phenomenon of increased firing frequency initially during prolonged stimulation ('negative adaptation') is an effect of the slow K^+ current inactivation being faster than the slow Na^+ current inactivation at comparable degrees of membrane polarization.

5. From further model studies it also appeared that, during depolarizations between successive action potentials evoked by constant stimulation, the membrane behaves like a high-resistance constant-current generator feeding into a short-circuiting capacitor. In consequence, the cell's stimulus sensitivity (change in firing frequency with stimulation strength) is, at functionally relevant stimulation intensities, mainly determined by the membrane capacitance and by the amplitude of the interspike membrane depolarization while, at higher stimulation intensities and firing frequencies, it becomes more and more a function of the spike duration itself.

INTRODUCTION

In an earlier series of investigations (Edman, Gestrelius & Grampp, 1983; Gestrelius & Grampp, 1983*a*, *b*; Gestrelius, Grampp & Sjölin, 1983) it has been shown that, in the slowly adapting stretch receptor neurone of lobster, the regulation of impulse firing is due to a specific setting of the control of membrane currents in near-threshold voltage regions. In particular, it could be demonstrated that the cell's 'slow' type of firing adaptation depends on a sluggish type of Na^+ and K^+ current inactivation, in combination with a slow Na^+-dependent pump current activation.

In order to see whether similar mechanisms of current control are also involved in firing regulation in the rapidly adapting receptor, this cell was examined with respect to its membrane current properties in the same way as had been done with the slowly adapting cell. Such a study seemed to be justified, since it is known from previous work (Gestrelius, Grampp & Sjölin, 1981) that the same kind of membrane currents do exist in the two receptor neurones.

The study was subdivided into two parts, the first of which has been published (Edman, Gestrelius & Grampp, 1986). It describes the cell's pump and leak current components, and it gives evidence that the kinetic properties of these currents cannot explain the receptor's specific firing behaviour. In this second part of the study, attention will be focussed on the cell's gated membrane currents and on their dynamic interaction in the process of firing regulation. The currents that will be analysed in this context are a tetrodotoxin-sensitive Na^+ current and a tetraethylammonium- and 4-aminopyridine-sensitive K^+ current. A Ca^{2+}-dependent K^+ current (C-current, Gestrelius *et al.* 1981) will, on the other hand, not be taken into further consideration. The reason for this is that the C-current is not positively identifiable in the slowly adapting receptor under drug-free conditions (Gestrelius & Grampp, 1983*b*) and, therefore, may only exist as a pharmacological artifact following 4-AP treatment (cf. Hermann & Gorman, 1981).

The main results of the present investigation are (a) that the gated membrane currents of the rapidly adapting cell can, after numerical modification of only a few control parameters, be described by exactly the same kinetic expressions as corresponding currents in the slowly adapting receptor, and (b) that a mathematical model, developed from the current measurements, is able to correctly reproduce the living receptor's firing activity as a function of both time and stimulation intensity. From the receptor model it is inferred that the cell's firing properties, in particular its 'rapid' mode of adaptation, are largely determined by a marked tendency to spike accommodation initiated by a slow type of Na^+ current inactivation.

Some aspects of the results to be described have been discussed in a doctoral thesis by one of the authors (Gestrelius, 1983).

METHODS

Preparation

All experiments were carried out on rapidly adapting stretch receptor neurones from the second and third abdominal segments of the European lobster (*Homarus gammarus*). For electrophysiological examination, stretch receptor organs were isolated and mounted in an experimental chamber which was continuously perfused with solutions of desired composition at 18 °C.

In order to obtain better voltage control in voltage-clamp measurements, the axon of the receptor neurones was ligated with a fine nylon thread at a distance of 600–800 μm from the cell body. In slowly adapting receptor neurones, where the axonal spike trigger zone is located about 200 μm from the cell body (Grampp, 1966), the ligation procedure was found to have no adverse effect on the cells' viability and firing behaviour, but could be assumed to provide satisfactory (at least 90 %) voltage control, even in the peripheral parts of the preparation (Gestrelius & Grampp, 1983*a*).

During the experiments, the receptor neurones were fully relaxed. Measurements were begun only after the cell's membrane voltage and input resistance had stabilized completely following micro-electrode impalement; this usually took 30–60 min.

Solutions

The standard saline solution used had the following composition (mM): NaCl, 325; KCl, 5; $CaCl_2$, 25; $MgCl_2$, 4; $MgSO_4$, 4; Tris HCl, 26; Tris base, 4; and glucose, 5; the pH of the solution was set to 7·3–7·4 by titrating with 0·5 M-NaOH after 20 min of bubbling with 5 % CO_2 in O_2. Test solutions containing tetrodotoxin (TTX) either alone or in combination with tetraethylammonium (TEA) and 4-aminopyridine (4-AP) were prepared fresh for each experiment. Picrotoxin (8·3 μM) was added to all solutions in order to suppress spontaneous miniature inhibitory post-synaptic potentials.

Membrane voltage and current measurements

Membrane voltage and current measurements were made with intrasomally placed double-barrelled micro-electrodes. Both barrels, of which one was used for voltage recording and the other for current passage, were filled with 3 M-KCl and had, after bevelling (as described by Clementz & Grampp, 1976), resistances of 6–8 MΩ. Conventional electronic equipment was employed for signal recording in both current- and voltage-clamp measurements. Voltage artifacts due to current passage through series resistances in the preparation and bath, and through capacitative coupling between the electrode barrels, were eliminated by signal subtraction from the output of the electrometer amplifier. The signals to be subtracted were obtained by appropriate amplification and filtration of the feed-back signals from the control amplifier. In voltage-clamp measurements the reference signal to the control amplifier was passed through a low-pass filter with a time constant of 20 ms (corresponding to a cut-off frequency of 8 Hz), in order to prevent (or delay) the activation of uncontrollably large membrane currents. With respect to this adjustment, the first 100 ms of membrane current responses to so-called 'voltage steps' were not taken into quantitative consideration.

The type of recording device described above had been found, in previous voltage-clamp tests (Gestrelius & Grampp, 1983*a*), to achieve a satisfactory (better than 95 %) control of currents up to $\pm$30 nA in a frequency range from d.c. to 500 Hz. The equipment was therefore considered suitable for a reliable estimation of membrane currents and their (slow) dynamics in sub- and near-threshold voltage regions, whereas, in clearly suprathreshold voltage regions, an assessment of current properties could only be obtained by inference from data in the literature and from computer simulation of the cells' recorded impulse activity.

Numerical methods

Mathematical simulation of empirical data was performed on a computer (CAI Alpha LSI 4/90) using a single precision version of a FORTRAN-based program for numerical integration of partitioned stiff ordinary differential equations and differential–algebraic systems, developed by Söderlind (1980).

RESULTS

Analysis of gated membrane currents

Of the two gated membrane currents examined in this study, the Na^+ current is defined as the difference between membrane currents recorded before and after treatment with 480 nM-TTX (Fig. 1*A*, inset), and the K^+ current as the difference between membrane currents recorded before and after treatment with 10 mM-TEA and 0·5 mM-4-AP in the continued presence of TTX (Fig. 2, inset). As in the slowly adapting receptor, both currents exhibited a slow inactivation during prolonged

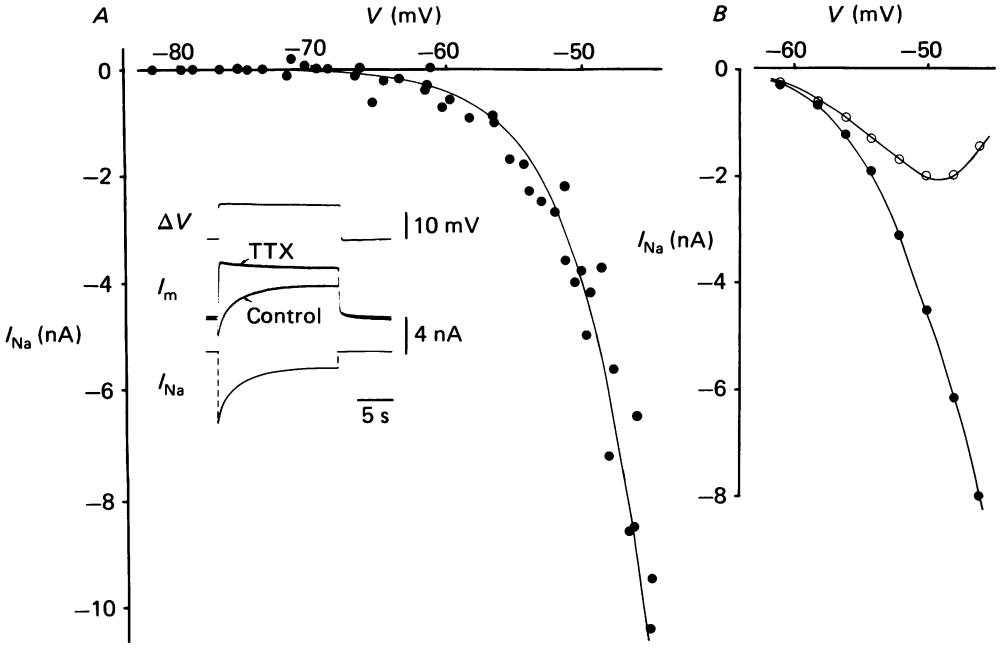

Fig. 1. *A*, inset, simultaneous recordings of change in membrane voltage, ΔV (relative to resting voltage at −61 mV), and membrane current, I_m, before and after treatment with 480 nM-TTX, as indicated. I_{Na}, estimate of Na^+ current obtained by subtracting the membrane current recordings, I_m, from each other. Graph, relationship between membrane voltage, V, and Na^+ current, I_{Na}, in the absence of slow Na^+ current inactivation. The points represent current responses recorded 100 ms after the onset of depolarizing test 'voltage steps' in seven different cells. The voltage steps were preceded by 10 s pulses of membrane hyperpolarization to −85 mV, in order to eliminate the slow Na^+ current inactivation. The curve is drawn according to eqn. (2) using relevant parameters in Tables 1 and 2. *B*, relationship between membrane voltage, V, and Na^+ current, I_{Na}, before (filled circles), and after full development of the slow Na^+ current inactivation (open circles). The smooth curves were drawn by eye.

pulses of membrane depolarization, and rapid turning-on and turning-off reactions in connexion with depolarizing or repolarizing 'voltage steps'. The rapid reactions were ascribed to Hodgkin–Huxley (1952) *m*-, *h*-, and *n*-processes, whereas the slow reactions were seen as signs of a so-called *l*-process in the case of the Na^+ current, and of an *r*-process in the case of the K^+ current, as in the slowly adapting cell (Gestrelius & Grampp, 1983*a*; Gestrelius *et al.* 1983). On this basis, it was assumed that the cell's gated membrane currents are, like their counterparts in the slowly adapting receptor (Gestrelius & Grampp, 1983*b*), appropriately described by the constant field equation and by gating kinetic expressions, as specified in the Appendix.

Starting from this assumption, attempts were made to define numerically the various parameters of the formal current descriptions. For the parameters of the fast *m*-, *h*-, and *n*-processes, and for the maximum Na^+ and K^+ permeabilities, values had to be inferred from data in the literature, from our own observations on the action

potential, and from measurements of the sub- and near-threshold Na^+ and K^+ currents in the absence of slow inactivation. Such measurements are illustrated in Figs. 1*A* and 2 in which the points represent current responses recorded 100 ms after the onset of 'voltage steps' of various heights from a holding level of about −85 mV, at which there is no slow current inactivation (see below).

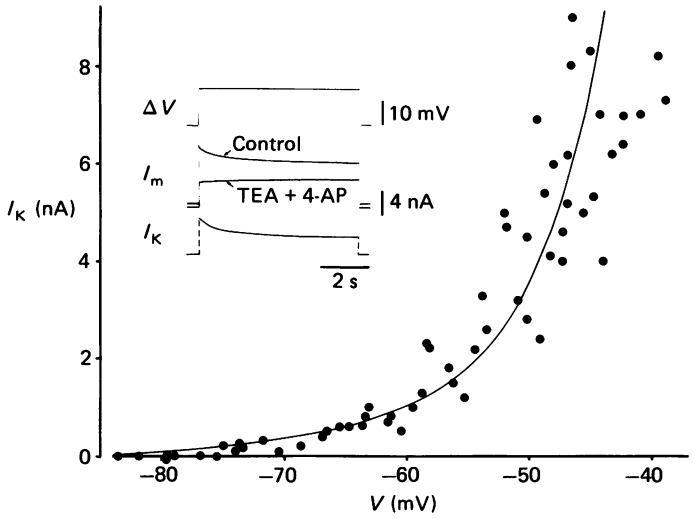

Fig. 2. Inset, simultaneous recordings of membrane voltage, ΔV (relative to resting voltage at −64 mV), and membrane current, I_m, in the presence of 480 nM-TTX before and after treatment with 10 mM-TEA + 0·5 mM-4-AP, as indicated. I_K, estimate of K^+ current obtained by subtracting the membrane current recordings, I_m, from each other. Graph, relationship between membrane voltage, V, and K^+ current, I_K, in the absence of slow K^+ current inactivation. The points represent current responses recorded 100 ms after the onset of depolarizing test 'voltage steps' in eight different cells. The voltage steps were preceded by 10 s pulses of membrane hyperpolarization to −85 mV, in order to eliminate the slow K^+ current inactivation. The smooth curve is drawn according to eqn. (3) using relevant parameters in Tables 1 and 2.

With regard to the Na^+ current, the various observations suggest that its activation is in suprathreshold voltage regions comparable to, but in sub- and near-threshold voltage regions clearly weaker than that of the slowly adapting cell. The latter fact is also indicated by the findings that there is a decline in steady-state Na^+ current with depolarizations beyond voltage levels of about −50 mV (Fig. 1*B*, open circles), and that there is no steady-state near-threshold TTX-sensitive membrane noise, unlike conditions in the slowly adapting receptor (Sjölin & Grampp, 1975). For the K^+ current, the experimental data show that it is, in both sub- and suprathreshold voltage regions, stronger than that of the slowly adapting receptor.

In the mathematical model, the observations presented above could be accounted for by assuming larger maximum Na^+ and K^+ permeabilities and a more positive mid-point voltage of the m_∞–voltage relationship (the subscript ∞ indicating steady-state value) but, for the rest, the same m-, h-, and n-parameters as in the slowly adapting receptor (Table 1). On the basis of these assumptions and the parameters

listed in Table 2, it was found that the model gave satisfactory reproductions of the cell's action potential (Fig. 5) as well as of its sub- and near-threshold Na^+ and K^+ currents (continuous lines in Figs. 1*A* and 2). An alternative choice of parameters involving a negative shift of the h_∞–voltage and n_∞–voltage relationship, also providing for a small ratio between subthreshold Na^+ and K^+ currents, was abandoned since it implied a very fast accommodative decrease in impulse height during repetitive firing which was simply not seen in living cells during moderately strong stimulation.

For the slow processes of Na^+ and K^+ current inactivation, parametric characterizations were obtained by measuring their steady-state values and their time constants as a function of membrane polarization in voltage ranges that could be kept under control by the recording equipment. The results of measurements of the steady-state degree of the slow inactivations are given in Figs. 3*A* and 4*A*. They are expressed in terms of gating variables, l and r, which reflect the relative amount of Na^+ current, or K^+ current, that could be activated by a test depolarization, V_t, after keeping the membrane voltage at various levels, V, long enough (10 s) for the slow inactivations to assume steady-state values.

Measurements of the time constants of the slow inactivations, τ_l and τ_r, are shown in Figs. 3*B* and 4*B*. The values were assessed directly (filled symbols) from the exponential decline of current responses to voltage steps as shown in the insets of Figs. 1*A* and 2, and indirectly (half-filled and open symbols) from the exponential decline of current responses to test depolarizations, V_t, with time, t, of membrane polarization at various voltage levels, V, as shown in Figs. 3*C* and 4*C*.

From the measurements, it appears that the l_∞–voltage and τ_l–voltage relationships are not significantly different from those obtained from the slowly adapting receptor (Gestrelius *et al.* 1983). The same l-parameters as had been inferred for this cell were therefore adopted for the present preparation. Their numerical values are listed in Table 1 and are implied in the predictions of eqns. (9) and (10) which are reasonably satisfactory reproductions of the experimentally observed relationships (continuous lines in Fig. 3*A* and *B*).

For the slow K^+ current inactivation, the measurements show that the process is, at all voltage levels, both faster and more complete than its counterpart in the slowly adapting receptor. Hence, a new set of r-parameter values was inferred according to principles described by Gestrelius & Grampp (1983*a*). The values are given in Table 1 and are also implied in the predictions of eqns. (9) and (10) which reproduce reasonably well the measured r_∞–voltage and τ_r–voltage relationships (continuous lines in Fig. 4*A* and *B*).

Analysis of firing control

Following characterization of the gated membrane currents, an attempt was made to find out whether or not their kinetics, together with those of other identified membrane currents, can explain the specific firing behaviour of the rapidly adapting receptor. This was done by substituting all current control parameters obtained in this and a preceding investigation (Table 2) into a mathematical model of the receptor and comparing the model's dynamic behaviour with that of the living cell. The results of this comparative study will be further discussed below.

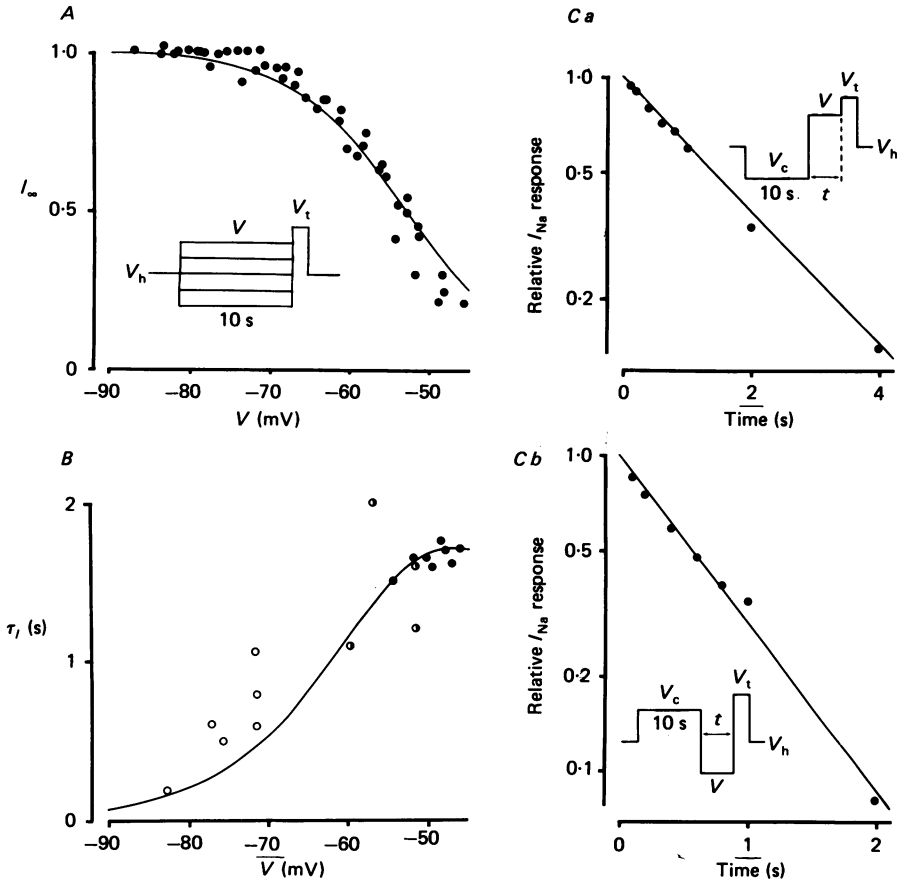

Fig. 3. *A*, relationship between membrane voltage, V, and steady-state degree of the slow Na^+ current inactivation, l_∞. The points represent measurements in seven different cells. Inset, experimental protocol according to which l_∞ was estimated from the relative height of Na^+ current responses to a test depolarization, V_t, following membrane polarization at various voltage levels, V, for 10 s. V_h, holding voltage, equal to resting voltage. The smooth curve is drawn according to eqn. (9) using relevant parameters in Table 1. *B*, relationship between membrane voltage, V, and time constant, τ_I, of the slow Na^+ current inactivation. The points represent measurements obtained directly (closed symbols, six different cells) from the exponential decay of Na^+ current responses to prolonged membrane depolarizations as shown in the inset of Fig. 1*A*, or indirectly (half-filled and open symbols, seven different cells) from the exponential change of Na^+ current responses to a test depolarization with duration of membrane polarization at various voltage levels as shown in panels *Ca* and *b*. The smooth curve is drawn according to eqn. (10) using relevant parameters in Table 1. *Ca* and *b*, examples of change of Na^+ current responses to a test depolarization, V_t, with time, t, of membrane polarization at a voltage level, V, as shown in the insets. In order to provide for clearly discernible effects of the slow Na^+ current inactivation at various voltage levels, the measurements were preceded by 10 s pulses of conditioning membrane hyperpolarization (*Ca*, half-filled symbols in *B*) or depolarization (*Cb*, open symbols in *B*), V_c. V_h, holding voltage, equal to resting voltage. The continuous line represents an exponential fit to the measured points.

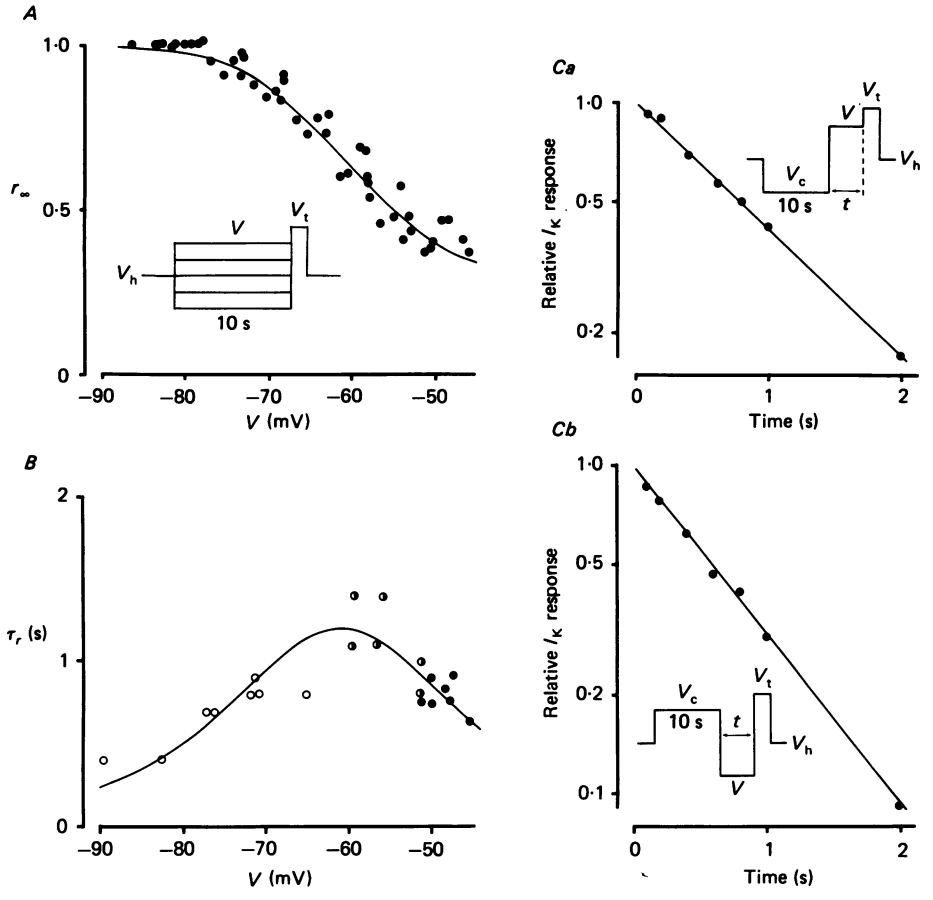

Fig. 4. *A*, relationship between membrane voltage, V, and steady-state degree of the slow K^+ current inactivation, r_∞. The points represent measurements in seven different cells. Inset, experimental protocol according to which r_∞ was estimated from the relative height of K^+ current responses to a test depolarization, V_t, following membrane polarization at various voltage levels, V, for 10 s. V_h, holding voltage, equal to resting voltage. The smooth curve is drawn according to eqn. (9) using relevant parameters in Table 1. *B*, relationship between membrane voltage, V, and time constant, τ_r, of the slow K^+ current inactivation. The points represent measurements obtained directly (closed symbols, six different cells) from the exponential decay of K^+ current responses to prolonged membrane depolarizations as shown in the inset of Fig. 2, or indirectly (half-filled and open symbols, eight different cells) from the exponential change of K^+ current responses to a test depolarization with duration of membrane polarization at various voltage levels as shown in panels *Ca* and *b*. The smooth curve is drawn according to eqn. (10) using relevant parameters in Table 1. *Ca* and *b*, examples of change of K^+ current responses to a test depolarization, V_t, with time, t, of membrane polarization at a voltage level, V, as shown in the insets. In order to provide for clearly discernible effects of the slow K^+ current inactivation at various voltage levels, the measurements were preceded by 10 s pulses of conditioning membrane hyperpolarization (*Ca*; half-filled symbols in *B*) or depolarization (*Cb*; open symbols in *B*), V_c. V_h, holding voltage, equal to resting voltage. The continuous line represents an exponential fit to the measured points.

TABLE 1. Gated ion channel parameters. The meaning of the various symbols is explained in the Appendix. Values differing from those assumed for the slowly adapting receptor are marked by an asterisk

Gating process (p)	δ_p	z_p	ν_p	$\bar{\tau}_p$ (ms)	V_p (mV)	$\bar{P}_{Na}$ (cm/s)	$\bar{P}_K$ (cm/s)
m	0·3	3·1	0·0	0·3	−13*	$5·6 \times 10^{-4}$*	—
h	0·5	−4·0	0·0	5·0	−35	—	—
l	0·3	−3·5	0·0	1700	−53	—	—
n	0·3	2·6	0·03	6·0	−18	—	$2·4 \times 10^{-4}$*
r	0·5*	−4·0	0·3*	1200*	−61*	—	—

TABLE 2. Current control parameters of the rapidly adapting stretch receptor neurone according to Edman *et al.* (1986). The values do not differ significantly from those inferred for the slowly adapting receptor except for the value of the maximum Na^+ extrusion capacity, marked by an asterisk

Cell geometry	
Membrane area (A)	$1·0 \times 10^{-3}$ cm^2
Cell volume (v)	$1·25 \times 10^{-6}$ cm^3
Resting intracellular ion concentrations	
$[Na^+]_{i,rest}$	10 mM
$[K^+]_{i,rest}$	160 mM
$[Cl^-]_{i,rest}$	46 mM
Resting membrane voltage	−65 mV
Passive membrane properties	
Specific membrane capacitance (C_m)	7·8 μF/cm^2
Leak permeabilities	
$P_{L,Na}$	$5·8 \times 10^{-8}$ cm/s†
$P_{L,K}$	$1·8 \times 10^{-6}$ cm/s
$P_{L,Cl}$	$1·1 \times 10^{-7}$ cm/s
α (fractional value of total K^+ leak)	0·87
Na^+–K^+ pump parameters	
Na^+–K^+ transport ratio	3 : 2
Maximum Na^+ extrusion capacity ($\bar{J}_{p,Na}$)	$3·0 \times 10^{-10}$ mol/(cm^2 s)*
Apparent Na^+-pump site dissociation constant (K_m)	7·7 mM†

† Values inferred by adjusting the model to resting conditions (see Appendix).

The mathematical model

The main purpose of the present study is to shed light on the mechanisms of firing control under conditions of prolonged stimulation. Therefore, as in an earlier investigation concerning firing control in the slowly adapting receptor (Gestrelius & Grampp, 1983*b*), the analysis is more concerned with the slow process of interspike membrane depolarization leading to spike initiation than with the details of the action potential itself. In the living cell, the process of spike initiation does take place in the axonal spike-trigger zone but is nevertheless dependent on the cell's integrated membrane properties since, with natural stimulation or stimulation by means of intrasomal current injection, the cell's soma-dendritic zone has to be depolarized first

before an action potential is set up in the spike-trigger region. On these grounds, it seemed justified to consider the receptor as an isopotential pace-maker structure, in which case its function was assumed to be adequately described by the Hodgkin–Huxley (1952) membrane equation (for details, see Appendix).

Comparison between recorded and simulated firing activities

Resting conditions. In both living receptors and in the model, resting conditions imply that all ionic membrane currents add up to zero at a membrane voltage of −65 mV (Table 2). In the model this adjustment is achieved according to principles explained in the Appendix.

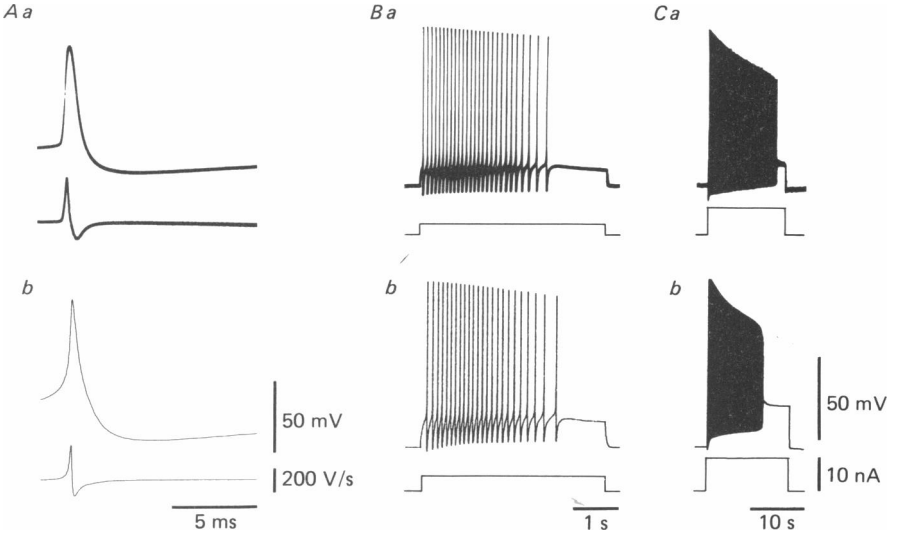

Fig. 5. *A*, intrasomally recorded (*a*) and mathematically simulated (*b*) action potentials (upper traces) and their time derivatives (lower traces). The action potentials represent the first impulses of low-frequency spike trains. *B* and *C*, intrasomally recorded (*Ba* and *Ca*) and mathematically simulated (*Bb* and *Cb*) spike trains (upper traces) evoked by prolonged square current pulses of different strengths (lower traces).

The individual action potential. In the living cell, action potentials were recorded during intrasomal injection of prolonged depolarizing current pulses. In the model, this situation was simulated by solving eqn. (1) after substituting a finite value for the stimulating current. The results of impulse recordings and firing simulations are illustrated in Fig. 5. In *Aa* and *Ab* individual recorded and simulated action potentials and their time derivatives in high time resolution are shown; in both cases the action potentials were taken from the beginning of low-frequency impulse trains. It is seen that the model reproduces the recorded action potential reasonably well with respect to height, duration and maximum rates of rise and fall. It fails, however, to reproduce the sudden onset of the recorded action potential since the model simulates a non-propagated type of pace-maker activity, while the recorded action potential is partly shaped by its propagation from the axonal spike-trigger zone into the cell's soma-dendritic region.

Repetitive impulse firing. Typical examples of repetitive firing in a living receptor at two different stimulation intensities are given in Fig. 5*Ba* and *Ca*. It thus appears that during maintained impulse activity there is a progressive decrease in spike height and in the depth of the spike after-hyperpolarization and a gradual fall in firing frequency. Characteristically, the impulse activity is terminated abruptly despite continued stimulation. In Fig. 5*Ba* and *Ca* it can be seen that the type of firing behaviour described above is closely simulated by the mathematical receptor model.

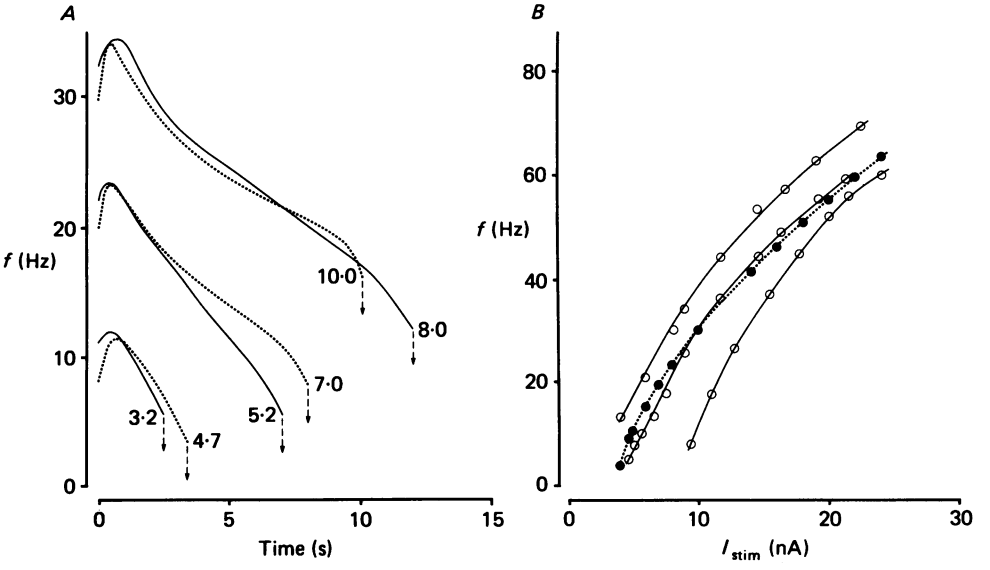

Fig. 6. *A*, firing frequency, *f*, as a function of time in a living receptor (continuous lines) and in the mathematical model (interrupted lines) at various constant stimulation intensities (given in nA beside each curve). Firing cessation is indicated by downwardly directed arrows. *B*, relationship between stimulation intensity, I_{stim}, and 'instantaneous' firing frequency (frequency of the first two spikes in each spike train), *f*, in the living receptor (three different cells marked by continuous lines) and the mathematical model (interrupted line).

In the following discussion, the observed agreement between recorded and simulated impulse activities serves as a basis for further analysis of repetitive firing as a function of time (adaptation) and stimulation intensity (stimulus sensitivity) both in the living preparation and in its mathematical model.

Frequency adaptation. In living rapidly adapting receptors, it is noted that there is a considerable variability in frequency adaptation. Thus, in some preparations adaptation is of an almost slow type, whereas in others it is extremely rapid, allowing only spike trains of a few seconds maximum duration. An example of an 'average' kind of adaptive behaviour at various stimulation intensities is given in Fig. 6*A* (continuous lines). It shows that during maintained stimulation the firing frequency falls, after an initial small increase, to progressively lower levels, until it drops to zero abruptly. The cut-off frequency levels tend to increase with the cell's initial firing rate. From the interrupted lines in Fig. 6*A*, it can be seen that the firing behaviour of the average living cell is successfully reproduced by the mathematical model.

Stimulus sensitivity. Operationally, stimulus sensitivity may be defined as change in 'instantaneous' firing frequency (frequency of the first two spikes in a spike train) with stimulation intensity. Several examples of experimentally observed relationships between stimulation intensity and 'instantaneous' firing frequency are given in Fig. 6*B* (continuous lines). They illustrate that, despite some variation in rheobase (minimum stimulation intensity required for repetitive firing), different receptors differ little with respect to their stimulus sensitivity (slope of the stimulus–frequency relationship). The fact that in all cells the stimulus sensitivity decreases with increasing firing frequencies is due to a finite spike length which sets an upper frequency limit at 120–150 Hz. As shown by the interrupted line in Fig. 6*B*, the computed stimulus sensitivity is in close agreement with that of the living cells, while the computed rheobase may differ from experimentally observed values. The reason for this discrepancy, as well as for any variation in rheobase between individual cells, is that there is a variation in resting membrane polarization because of somewhat differently adjusted pump and leak current kinetics.

Model analysis of the mechanisms of firing control

From the findings above it appears that the model is reasonably well able to simulate impulse firing of the rapidly adapting receptor under different functional circumstances. Hence, it seemed to be justifiable to adopt it as a plausible theory of cellular firing control and to use it for further exploration of this function. In the following sections, this will be done by studying the effects of manipulating some of the model's parameters on its firing behaviour.

Spike configuration during repetitive firing. For an analysis of the mechanisms underlying changes in spike configuration during repetitive firing, the slow processes of Na^+ and K^+ current inactivation were in the model locked at their resting values during prolonged impulse activities. From the effects of this investigation, it was obvious that the gradual decline in spike height during repetitive firing is primarily an effect of the slow Na^+ current inactivation, while the progressive decrease of the spike after-hyperpolarization is caused mainly by the slow K^+ current inactivation but also, to some extent, by a reduction in K^+ current activation following the decline in impulse height.

Frequency adaptation. In order to estimate the mechanisms of firing adaptation, impulse firing was simulated before and after re-adjustment of some critical control parameters. The results of these experiments are given in Fig. 7*A*, where the firing frequency is shown as a function of time during constant stimulation. It can be seen that the phenomenon of 'rapid' adaptation, including abrupt firing cessation, can be abolished by locking the slow Na^+ current inactivation (at its resting level) and/or by shifting the m_∞–voltage relationship slightly (2 mV) in a negative direction. From this it follows that the occurrence of 'rapid' adaptation is essentially the result of a slow Na^+ current inactivation. This reaction further decreases an already limited capacity for near-threshold Na^+ current activation (see above), and thereby initiates a regenerative cycle of spike accommodation, leading to a progressive weakening and ultimate extinction of the depolarizing interspike membrane current (Fig. 8*C*). As a matter of course, these changes give rise to an initial decrease and final drop to zero of the firing frequency.

In this context, it should be noted that even after substantial reduction of the depolarizing interspike membrane current there is still a considerable potential for spike current production. This is illustrated in Fig. 8*B* (current loop *b*) and is evident also from the fact that, especially after short-lasting fully adapted spike trains, it is possible to re-initiate impulse firing in the living preparation, as well as in its mathematical model, by increasing the stimulation intensity by relatively small amounts (Fig. 9*A*).

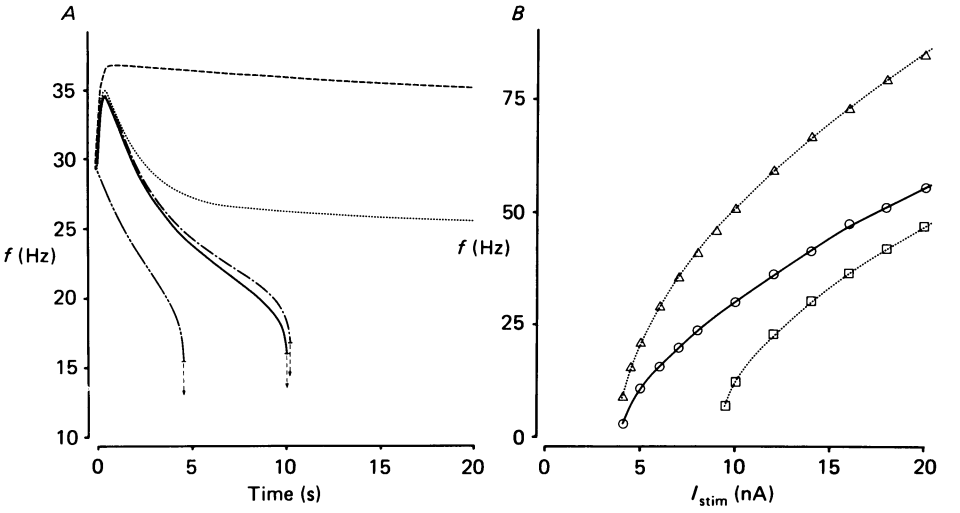

Fig. 7. *A*, simulated firing frequency, *f*, as a function of time during constant stimulation in control conditions (——); after individually locking, at their resting values, the slow Na^+ current inactivation (– – –), the slow K^+ current inactivation (— · —), and the Na^+-dependent pump current activation (— · —); and after shifting the m_∞–voltage curve by 2 mV in a negative direction (------). Firing cessation is indicated by horizontal bars and downwardly directed arrows. *B*, simulated relationships between stimulation intensity, I_{stim}, and 'instantaneous' firing frequency (frequency of the first two spikes in each spike train), *f*, in control conditions (circles); and after halving the membrane capacitance (triangles), or doubling the K^+ leak permeability (squares). The continuous and interrupted lines were drawn by eye.

A further phenomenon shown in Fig. 7*A* is that locking the pump current generation (at its resting value) has only minor effects on the model's firing behaviour. This is understandable on the ground that the pump mechanism is not normally much activated by spike firing whose rapid adaptation prevents intracellular accumulation of Na^+ in significant amounts.

Finally, it appears from Fig. 7*A* that locking the slow K^+ current inactivation (at its resting value) eliminates the initial increase in firing frequency, reminiscent of the so-called 'negative adaptation' in e.g. dorsal spinocerebellar tract neurones (Gustafsson, Lindström & Zanger, 1978). Thus, in the lobster stretch receptor neurone, the presence of this phenomenon can be ascribed to the existence of a slow K^+ current inactivation which, at near-threshold voltage levels, is distinctly faster than the slow Na^+ current inactivation. In conditions of near-rheobase stimulation, this type of

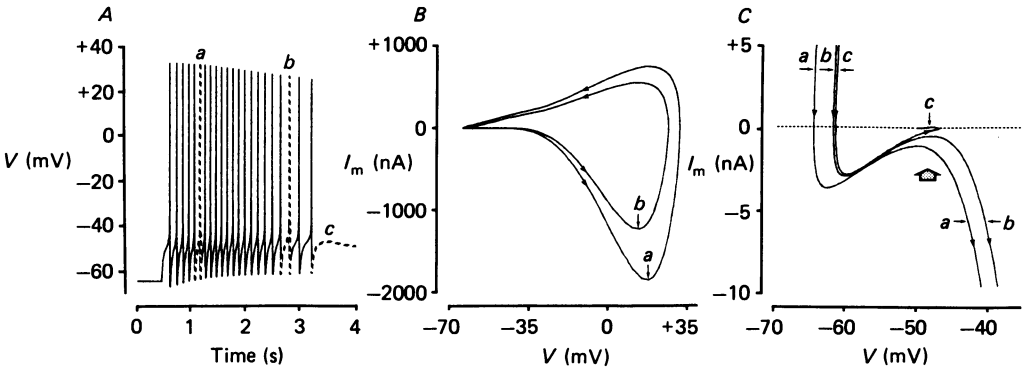

Fig. 8. *A*, simulated spike train during constant stimulation (*V*, membrane voltage). The interrupted sections of the tracing indicate events that are also represented in *B* and *C*. *B*, simulated relationships between membrane voltage, *V*, and membrane current, I_m, during complete spike cycles that are marked *a* and *b* in *A*. *C*, simulated relationships between membrane voltage, *V*, and the interspike and post-spike membrane current, I_m, pertaining to events marked *a*, *b*, and *c* in *A*. The vertical arrow indicates the gradual shift of the interspike membrane current towards zero value (horizontal interrupted line).

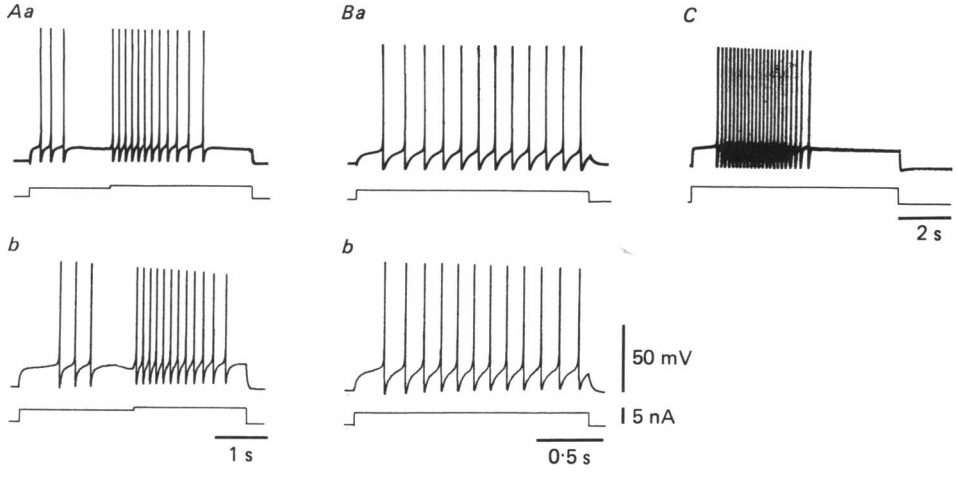

Fig. 9. *A*, intrasomally recorded (*a*) and mathematically simulated (*b*) impulse activities (upper traces) evoked by stepwise increasing stimulation intensities (lower traces). *B* and *C*, intrasomally recorded (*Ba* and *C*) and mathematically simulated (*Bb*) impulse activities (upper traces) evoked by prolonged square-wave current pulses (lower traces); the recordings illustrate a delay in firing onset and an initial increase in firing frequency. *Ba* and *C* refer to different cells.

current control gives rise to a delay in firing onset which can be seen both in model responses and in the living receptor, where it may sometimes assume considerable proportions (Fig. 9*B* and *C*).

Stimulus sensitivity. According to the definitions above, stimulus sensitivity is a function of the 'instantaneous' firing frequency. The 'instantaneous' firing frequency is, in turn, a function of the duration of the first action potential and of the first spike

interval in a spike train. Of these two durations, it is mainly the latter which can be modified by variations of the stimulation intensity. Its determinant factors were, therefore, made the object of a more detailed model analysis.

In this analysis, the interspike membrane current, ranging between zero (at the bottom of the first spike after-hyperpolarization) and −30 nA (around 'threshold' of the second action potential), was plotted as a function of both time and membrane polarization (Fig. 10). From these plots, it appears that the interspike membrane

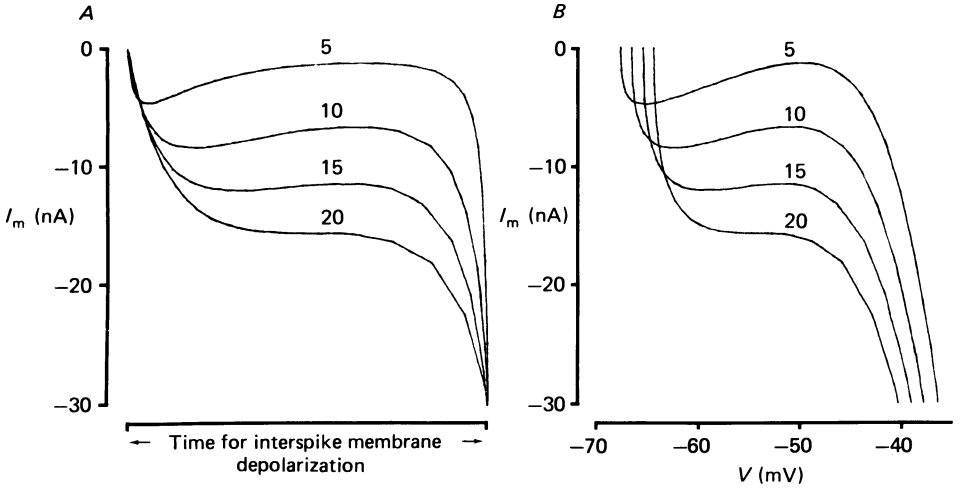

Fig. 10. Simulated membrane current, I_m, during the first spike interval in a spike train as a function of time (*A*) and of membrane voltage (*V*; *B*) at different stimulation intensities (given in nA beside each curve). For further details, see text.

current increases roughly in proportion to the stimulation intensity and that the amplitude of the interspike membrane depolarization is in the order of 30 mV, decreasing somewhat with increasing stimulation intensity. Furthermore, it is seen that the membrane current stays rather constant at all stimulation strengths over a substantial part of the spike interval (Fig. 10*A*) and varies only little within a fairly wide (about 20 mV) voltage range (Fig. 10*B*). From this it can be concluded that, during the interspike membrane depolarization, all sources of transmembrane ion currents (including the leak channel and internal or external generator or stimulating current sources) are combined into a high-resistance constant-current generator and that, in such circumstances, the output of this generator is fed into what appears to be a pure membrane capacitor and not an R–C network, as is sometimes assumed.

If correct, the above conclusion would imply that the time needed to depolarize the capacitor from maximum polarization to firing threshold, or the corresponding frequency of repetitive spike initiations, depends on the constant-current generator output, the amplitude of the interspike membrane depolarization and the membrane capacitance, but not on the membrane's leak permeability. In order to test this possibility, stimulus–firing-frequency relationships were simulated before and after halving the membrane capacitance, or doubling the leak permeability, respectively. The results are shown in Fig. 7*B*, where it can be seen that the slope of the observed

relationships (stimulus sensitivity) is distinctly affected by varying the membrane capacitance, but very little so by varying the leak permeability. That there are changes in stimulus rheobase concurrent with changes in leak permeability can be explained as a result of varying the load on the generator or stimulating-current source.

It thus appears that there is support for the above concept of interspike membrane function, from which it follows that the cell's stimulus sensitivity is, at moderate firing frequencies, determined both by the size of the membrane capacitance and the amplitude of the interspike membrane depolarization. The latter parameter, in turn, is determined by the cell's control of its gated membrane currents. At higher firing frequencies, it is obvious that the duration of the action potential itself becomes an increasingly dominating factor in determining the cell's stimulus sensitivity (see above).

DISCUSSION

In the present study an attempt was made to find kinetic expressions for the gated membrane currents of the rapidly adapting lobster stretch receptor neurone and to use these expressions in the formulation of a mathematical receptor model designed to explain the cell's specific firing behaviour. From the results it appears, first, that the currents investigated can be described by kinetic expressions which, except for a few parameter values, are identical with those previously inferred for the slowly adapting receptor; secondly, that the model formulated is able to correctly reproduce impulse firing in the living preparation and, thirdly, that the model can be used to explain the mechanisms behind the cell's firing behaviour in different functional circumstances. These points will be discussed in detail below.

Control of gated membrane currents

Typically, the gated Na^+ and K^+ currents are controlled, in the rapidly adapting receptor, in such a way that the ratio between them is relatively low, both in subthreshold voltage regions and during the falling phase of the action potential. This adjustment, which is reminiscent of standard conditions in invertebrate peripheral axons, provides for the production of fast action potentials, but also for a considerable tendency to accommodation. It is especially this latter property which distinguishes the rapidly adapting cell from its slowly adapting counterpart and, in fact, proves to be the main cause of its 'rapid' form of adaptation.

The control mechanisms underlying the observed current-balance closely resemble those identified in the slowly adapting cell. They appear to differ only by operating on larger maximum Na^+ and K^+ permeabilities, and by employing a more positively placed m_∞–voltage relationship. Of these two differences, the former may suggest that the rapidly adapting receptor has a higher ion-channel density than its slowly adapting counterpart, while the latter indicates that a cell's accommodative properties are most critically dependent on the setting of its gating system for Na^+ current activation.

A further clear difference is in the process of slow K^+ current inactivation which is both faster and more pronounced in the rapidly than in the slowly adapting receptor. The reason for this differentiation is not obvious. However, the very fact

that it can be demonstrated in preparations which do not seem to differ with respect to their cell surface anatomy (Edman *et al.* 1986) may be taken as strong evidence that the slow K^+ current inactivation represents a genuine membrane function, and is not merely a sign of pericellular K^+ accumulation. The latter possibility is also contradicted by the fact that the decreases in outward current occurring during slow K^+ current inactivation do not, after cessation of the membrane depolarization, leave behind any losses in outward current (tails of inward current) that could be attributed to a transmembrane K^+ re-distribution (cf. Fig. 2 and Gestrelius & Grampp, 1983*a*).

The mathematical receptor model

The rapidly adapting receptor model does not differ in structure from its slowly adapting counterpart. This means that it describes the cell as a homogeneous and not as a regionally (e.g. with respect to an axonal spike-trigger function) differentiated pace-maker unit. However, despite this simplifying assumption the model is, nevertheless, able to correctly reproduce the firing activity of the living preparation. This can be explained on the grounds that, as in the slowly adapting receptor (Gestrelius & Grampp, 1983*b*), impulse initiation is largely dependent on the cell's integrated membrane properties and that, after intrasomal measurements, these are properly represented in the model formulations.

Control of repetitive impulse firing

Using the model as a tool in a more detailed analysis of the mechanisms behind firing regulation, it was found that the cell's 'rapid' form of frequency adaptation depends on the slow Na^+ current inactivation which, with a gradually increasing involvement of the h- and n-mechanisms, leads to progressive throttling of the depolarizing inward current, until it is finally depressed below a critical level for spike initiation. Thus, firing adaptation can be seen as a process of slow accommodation which in the rapidly adapting cell always proceeds to completion because of its positively placed m_∞–voltage relationship, while it may stay incomplete in the slowly adapting receptor with its much wider margin of safety for the regenerative production of inward membrane current in near-threshold voltage regions.

In view of this functional arrangement, it seems clear that minor variations in the cell's current balance, e.g. due to shifts in the voltage dependence of the fast gating mechanisms or differences in cell size or leak permeability, will affect the slowly adapting receptor only by slightly modifying the degree of firing adaptation, whereas in the rapidly adapting cell it gives rise to marked changes in the duration of repetitive impulse activities. However, such a variability may not be of any functional significance since, in the living animal, the rapidly adapting receptor responds only to strong flexions of the abdomen, in which case it gives off a few spikes whose number and frequency is then largely determined by the rate of development and adaptation of the generator current (Eyzaguirre & Kuffler, 1955; Eckert, 1961; Nakajima & Onodera, 1969).

Considering its special mode of normal operation, it is also understood that the rapidly adapting cell is in no need of a very strong Na^+–K^+ pump (cf. Edman *et al.* 1986) nor of a precise setting of its slow K^+ current inactivation. That this setting may be quite variable is evident from the fact that individual cells differ considerably

with respect to the prominence of the phenomenon of 'negative adaptation' for which there is, as yet, no plausible functional explanation.

APPENDIX

A mathematical receptor model

Transmembrane current balance. The transmembrane current balance is described by the Hodgkin–Huxley (1952) membrane equation, according to which

$$\frac{dV}{dt} = -\frac{1}{AC_m}(I_{Na} + I_K + I_{L,Na} + L_{L,K} + I_{L,Cl} + I_p + I_{stim}). \quad (1)$$

In this equation dV/dt is the time derivative of the membrane voltage (inside minus outside), A is the projected membrane area, C_m is the specific membrane capacitance, I_{Na} and I_K are gated Na^+ and K^+ currents, $I_{L,Na}$, $I_{L,K}$, and $I_{L,Cl}$ are leak current components carried by Na^+, K^+, and Cl^-, respectively, I_p is a pump current, and I_{stim} is the stimulating current which, like all other currents, is given in units of current per cell.

The gated membrane currents are defined as

$$I_{Na} = A\bar{P}_{Na} m^2 h l \frac{VF^2}{RT} \frac{[Na^+]_o - [Na^+]_i \exp(FV/RT)}{1 - \exp(FV/RT)}, \quad (2)$$

and

$$I_K = A\bar{P}_K n^2 r \frac{VF^2}{RT} \frac{[K^+]_o - [K^+]_i \exp(FV/RT)}{1 - \exp(FV/RT)}, \quad (3)$$

where $\bar{P}_{Na}$ and $\bar{P}_K$ denote the maximum permeabilities for Na^+ and K^+, $[Na^+]_o$ and $[K^+]_o$ the extracellular, and $[Na^+]_i$ and $[K^+]_i$ the intracellular Na^+ and K^+ concentrations, and F, R, and T are the Faraday constant, the universal gas constant, and the absolute temperature, respectively. m, h, and l are gating variables describing the Na^+-channel activation and its fast and slow inactivation; and n and r are gating variables describing the K^+-channel activation and its slow inactivation.

The leak current components are expressed as

$$I_{L,J} = AP_{L,J} \frac{VF^2}{RT} \frac{[J]_o - [J]_i \exp(z_J FV/RT)}{1 - \exp(z_J FV/RT)}, \quad (4)$$

where J denotes any of the leak-current-carrying ions with valency, z_J, and extra- and intracellular concentrations, $[J]_o$ and $[J]_i$; and $P_{L,J}$ is the leak channel permeability for the ion, J.

The pump current is, in accordance with Garay & Garrahan (1973), defined as

$$I_p = \frac{AF}{3} \frac{\bar{J}_{p,Na}}{\left(1 + \frac{K_m}{[Na^+]_i}\right)^3}, \quad (5)$$

where $\bar{J}_{p,Na}$ represents the maximum Na^+ extrusion capacity of the Na^+–K^+ pump (in numbers of particles per area and time), K_m the apparent dissociation constant of each of three kinetically non-interacting Na^+-pump site complexes, and the factor

1/3 indicates that the net pump current is, because of the pump's 3:2 Na^+–K^+ transport ratio, only a third of the outwardly directed Na^+-pump current component.

The stimulating current, I_{stim}, is any current that does not directly affect the intracellular Na^+ concentration. As in experiments with living cells, it can be assumed to be carried by K^+ and Cl^-, whose intracellular concentrations are indirectly controlled by the cell's Na^+ transport system (Edman *et al.* 1986).

Transmembrane ion balance. For resting conditions, it is assumed that the intracellular concentrations of Na^+, K^+, and Cl^- are identical with their resting values, $[Na^+]_{i,rest}$, $[K^+]_{i,rest}$ and $[Cl^-]_{i,rest}$, as listed in Table 2.

For dynamic conditions, the internal Na^+ concentration can be computed from the continuity relationship

$$\frac{d[Na^+]_i}{dt} = -\frac{1}{Fv}(I_{Na} + I_{L,Na} + I_{p,Na}), \tag{6}$$

assuming that $[Na^+]_i = [Na^+]_{i,rest}$ at $t = 0$. In eqn. (6), $d[Na^+]_i/dt$ is the time derivative of the intracellular Na^+ concentration, v is the cell volume, and $I_{p,Na}$ is the Na^+ component of the pump current, which can be obtained from eqn. (5).

Since, according to Edman *et al.* (1986),

$$[Cl^-]_i = [Cl^-]_{i,rest} = \text{constant}, \tag{7a}$$

it follows from the principle of macroscopic electroneutrality that

$$[K^+]_i = [K^+]_{i,rest} - ([Na^+]_i - [Na^+]_{i,rest}). \tag{7b}$$

Channel gating kinetics. The various processes of channel gating are, in general terms, defined by the differential equation

$$\frac{dp}{dt} = (p_\infty - p)\frac{1}{\tau_p}, \tag{8}$$

where p represents any of the gating variables, m, h, l, n, or r, p_∞ its steady-state value, and τ_p the time constant of the gating process denoted. For the last two parameters it holds that, in accordance with Gestrelius & Grampp (1983*a*),

$$p_\infty = \nu_p + \frac{1-\nu_p}{1+\exp\left[\frac{z_p e}{kT}(V - V_p)\right]}, \tag{9}$$

and

$$\tau_p = \frac{Q_p \bar{\tau}_p}{\exp\left[\frac{\delta_p z_p e}{kT}(V - V_p)\right] + \exp\left[\frac{(\delta_p - 1) z_p e}{kT}(V - V_p)\right]}, \tag{10a}$$

where

$$Q_p = \left(\frac{1-\delta_p}{\delta_p}\right)^{\delta_p} + \left(\frac{1-\delta_p}{\delta_p}\right)^{\delta_p - 1}. \tag{10b}$$

In these expressions ν_p represents the minimum value of the relative channel permeability, z_p the effective valency of the gating structure, e the electron charge, and k the Boltzmann constant. V_p is the membrane voltage at which half of the gating

system is in its 'open' state, $\bar{\tau}_p$ the maximum value of the time constant τ_p, and δ_p the degree of energy barrier asymmetry with values varying between 0 and 1 (in the case of perfect barrier symmetry, $\delta_p = 0{\cdot}5$ and $Q_p = 2$).

Adjustment of the model to resting conditions. For resting conditions it holds that

$$I_{Na} + I_K + I_{L,Na} + I_{L,K} + I_{L,Cl} + I_p = 0, \quad (11)$$

at a resting voltage of −65 mV (according to measurements shown in Table 2). All currents in eqn. (11) are in principle defined by eqns. (2)–(5) and the parameter values inferred in this and in a preceding (Edman *et al.* 1986) study. For the leak and pump currents it holds, however, that their parameters were obtained under the simplifying assumption that the gated membrane currents are negligibly small in resting conditions. Since this is not in exact agreement with the findings of this investigation, some of the previously inferred parameter values have to be modified slightly in adjusting the model to resting conditions in order to comply with eqn. (11). The parameters chosen for this purpose are the Na^+ leak permeability, $P_{L,Na}$, and the apparent Na^+ dissociation constant of the pump, K_m. The reason for choosing these parameters is that modifying them slightly does not significantly alter the model's resting input resistance and its relationship between intracellular Na^+ concentration and the pump current production. It means only that elimination of the gated membrane currents leads to a positive shift of the model's resting voltage by slightly more than 1 mV. A similar depolarization can also be seen in living cells whose gated membrane currents have been blocked by TTX, TEA, and 4-AP.

To achieve a numerical adjustment of the parameters mentioned, it is assumed that, as a consequence of a 3:2 Na^+–K^+ active transport ratio,

$$(I_{Na} + I_{L,Na})/(I_K + \alpha I_{L,K}) = -1{\cdot}5, \quad (12)$$

at −65 mV (resting voltage), α denoting a fractional value of the total K^+ leak (for details, see Edman *et al.* 1986). After solving this equation for $I_{L,Na}$ and substituting the solution into eqns. (4) and (11) values for $P_{L,Na}$ and I_p are obtained. By substituting the computed value of I_p into eqn. (5) a value for K_m is also found.

The authors wish to express their gratitude to Ms Kristina Borglid for skilful technical assistance. The work has been supported by the Swedish Medical Research Council (project No. 2082) and by grants from the Medical Faculty of the University of Lund.

REFERENCES

CLEMENTZ, B. & GRAMPP, W. (1976). A method for rapid bevelling of micropipette electrodes. *Acta physiologica scandinavica* **96**, 286–288.

ECKERT, R. O. (1961). Reflex relationship of the abdominal stretch receptors of the crayfish. I. Feedback inhibition of the receptors. *Journal of Cellular and Comparative Physiology* **57**, 149–162.

EDMAN, Å., GESTRELIUS, S. & GRAMPP, W. (1983). Intracellular ion control in lobster stretch receptor neurone. *Acta physiologica scandinavica* **118**, 241–252.

EDMAN, Å., GESTRELIUS, S. & GRAMPP, W. (1986). Transmembrane ion balance in slowly and rapidly adapting lobster stretch receptor neurones. *Journal of Physiology* **377**, 171–191.

EYZAGUIRRE, C. & KUFFLER, S. W. (1955). Processes of excitation in the dendrites and in the soma of single isolated sensory nerve cells of the lobster and crayfish. *Journal of General Physiology* **39**, 87–119.

GARAY, R. P. & GARRAHAN, P. J. (1973). The interaction of sodium and potassium with the sodium pump in red cells. *Journal of Physiology* **231**, 297–325.

GESTRELIUS, S. (1983). Control of impulse firing in lobster stretch receptor neurones. *Acta physiologica scandinavica supplementum*, **513**, 1–15.

GESTRELIUS, S. & GRAMPP, W. (1983*a*). Kinetics of the TEA and 4-AP sensitive K^+ current in the slowly adapting stretch receptor neurone. *Acta physiologica scandinavica* **118**, 125–134.

GESTRELIUS, S. & GRAMPP, W. (1983*b*). Impulse firing in the slowly adapting stretch receptor neurone of lobster and its numerical simulation. *Acta physiologica scandinavica* **118**, 253–261.

GESTRELIUS, S., GRAMPP, W. & SJÖLIN, L. (1981). Subthreshold and near-threshold membrane currents in lobster stretch receptor neurones. *Journal of Physiology* **310**, 191–203.

GESTRELIUS, S., GRAMPP, W. & SJÖLIN, L. (1983). Kinetics of the TTX sensitive Na^+ current in the slowly adapting lobster stretch receptor neurone. *Acta physiologica scandinavica* **118**, 135–140.

GRAMPP, W. (1966). The impulse activity in different parts of the slowly adapting stretch receptor neurone of the lobster. *Acta physiologica scandinavica supplementum*, **262**, 1–36.

GUSTAFSSON, B., LINDSTRÖM, S. & ZANGER, P. (1978). Firing behaviour of dorsal spinocerebellar tract neurones. *Journal of Physiology* **275**, 321–343.

HERMANN, A. & GORMAN, A. L. F. (1981). Effects of 4-aminopyridine on potassium currents in a molluscan neurone. *Journal of General Physiology* **78**, 63–68.

HODGKIN, A. L. & HUXLEY, A. F. (1952). A quantitative description of membrane current and its application to conduction and excitation in nerve. *Journal of Physiology* **117**, 500–544.

NAKAJIMA, S. & ONODERA, K. (1969). Adaptation of the generator potential in the crayfish stretch receptor under constant length and constant tension. *Journal of Physiology* **200**, 187–204.

SJÖLIN, L. & GRAMPP, W. (1975). Membrane noise in slowly adapting stretch receptor neurone of lobster. *Nature* **257**, 696–697.

SÖDERLIND, G. (1980). DASP3 – a program for the numerical integration of partitioned stiff ODE:s and differential-algebraic systems. Report TRITA-NA-8008. Stockholm: Royal Institute of Technology.